

Flexible manipulation of the Goos-Hänchen shift in a cavity optomechanical systemMuhib Ullah ¹, Adeel Abbas,¹ Jun Jing,^{1,2} and Li-Gang Wang ^{1,2,*}¹*Department of Physics, Zhejiang University, Hangzhou 310027, China*²*Zhejiang Province Key Laboratory of Quantum Technology and Device, Zhejiang University, Hangzhou 310027, China*

(Received 15 October 2019; published 19 December 2019)

We propose a flexible manipulation on the Goos-Hänchen shift (GHS) via a cavity optomechanical system driven by an external coherent control field and reveal the behavior of the GHS as a result of light-matter interaction. It is achievable for both positive and negative GHSs in our system by tuning the coherent control field strength. The positive shift can flexibly be tuned to a negative shift by changing the cavity length. Furthermore, the control field can be used as a knob to turn the optical cavity on and off for manipulating the GHSs. A devastating suppression of the GHS can be observed due to weaker interaction between the cavity photons and the mechanical resonator by increasing the cavity decay rate. The results have potential applications in light-light manipulation via cavity optomechanical systems.

DOI: [10.1103/PhysRevA.100.063833](https://doi.org/10.1103/PhysRevA.100.063833)**I. INTRODUCTION**

The Goos-Hänchen shift (GHS) is a well-known optical phenomenon that appears when a classical electromagnetic light beam reflects from the interface of two optically different media. It is actually a lateral shift of reflected light beam from the actual point of reflection at the interface inferred by the geometrical optics rules, which was predicted for the first time by Picht [1]. The name “Goos-Hänchen shift” has been given in honor of Goos and Hänchen, the discoverers of the GHS in a total internal reflection experiment using a glass slab [2,3]. Artmann explained the GHS theoretically using the stationary phase method [4], and Renard explained it by the energy flux method [5]. The GHS has magnificent applications in optical switching [6], optical sensors [7–9], beam splitters [10], and optical temperature sensing [11], and it is enormously important regarding the theory of waveguides [12]. The GHS can be positive or negative depending upon the media used, such as weak absorbing media [13], weakly absorbing dielectric slab [14,15], gain media [16], negative refractive media [17,18], left-handed media [19–21], photonic crystals [22,23], and some other artificial materials [11,24–29]. Different optical structures, such as lossy or lossless slabs, have also been used to investigate the GHS [14,24].

Scully, in 1991, proposed a scheme to modify the two-level atomic susceptibility (dispersion-absorption relation) with a coherently prepared ground-state doublet using coherent control field [30]. To flexibly control the GHS in a fixed system, Wang *et al.* proposed a scheme to control the lateral shift by using a two-level atomic medium via a classical coherent control field [31]. Later on, Ziauddin *et al.*, in 2010, replaced the two-level atomic medium by three- and four-level atomic media with electromagnetically induced transparency to investigate the GHS for both reflected and transmitted probe

beams by adjusting the intensity of the control field. They reported that in the four-level configuration, positive as well as negative GHS can be enhanced with almost zero absorption [32]. Su *et al.* investigated the sensitivity of the GHS in a four-level atomic medium that can be controlled via two external coherent fields [33]. Moreover, Bacha *et al.* also used four-level atomic medium in an optical cavity to investigate the enhancement of the GHS in the region of spectral hole burning with and without the Doppler broadening effect [34]. Using a Δ configuration of the atomic medium, Deng *et al.* manipulated the GHS via electromagnetically induced transparency and amplification (EITA), which could result in positive as well as negative enhancements of the GHS by tuning the frequency of the probe field around EITA [35]. They showed that the GHS could be switched between considerably large positive and negative values by adjusting the collective phase of the external fields.

From the above discussion, we noted various schemes with different atomic level configurations or some dispersive media excited by external classical fields. An interesting idea from the cavity optomechanics is that nonlinearity can be introduced to an optomechanical system if it is excited by a strong coherent control field. This nonlinearity occurs due to the interaction between the cavity field and the mechanical mirror or resonator (light-matter interaction), which can lead to the modification of the effective refractive index of the cavity. It is very fascinating to investigate the manipulation of the GHS via a coherent control field in such a system as it provides us much flexibility to control the lateral shift. Instead of putting any media in a fixed cavity and modifying its susceptibility, we take a cavity optomechanical system (COMS) with a mechanical resonator (MR) and drive it with a coherent external control field, which has the tendency to modify the effective mechanical susceptibility χ_{eff} by changing its dynamics. It is very interesting to show the dependency of the GHS (which has a classical nature) on the cavity parameters (having quantum nature). Both positive and negative GHSs can be observed in the COMS by tuning the control field

*sxwlg@yahoo.com

and other cavity parameters for a certain incident angle of the probe light beam.

A single COMS comprises an optical cavity with a MR (perfectly reflecting) that has the tendency to control the dynamics of MR with the incoming driving control field [36–40]. The idea that a light field can impart momentum (in the form of radiation pressure) to material objects, such as MR, was given by Maxwell, and, in 1901, the radiation pressure of light was observed experimentally [41,42]. By changing the MR's dynamics using a coherent control field, its effective mechanical susceptibility χ_{eff} is changed, and thus, the dispersion-absorption relation of the cavity is modified [43]. That is what we need for the GHS in our COMS.

The makeup of this article is as follows: In Sec. II, we present the COMS model to find the GHS in the reflected probe light beams incident on the interface. Furthermore, we get the analytical results for the reflection coefficient and GHS, and we solve the system Hamiltonian to get the expression for χ_{eff} . In Sec. III, we analyze and discuss our results numerically, and, in the last section, there is a summary.

II. THE MODEL AND THEORY

We consider a COMS with a perfectly reflecting MR at its right side shown in Fig. 1, where δx is the mean displacement of MR from its equilibrium position. The left partially reflecting nonmagnetic mirror M is fixed, having thickness d_1 and permittivity ϵ_1 , whereas d_2 and ϵ_2 account for the effective cavity length and effective cavity permittivity, respectively. In Fig. 1, the optical cavity is driven by a strong classical coupling or control field (strength Ω_L , frequency ω_L) and a weak probe field (strength Ω_p , frequency ω_p), which is incident from vacuum ($\epsilon_0 = 1$) upon the COMS making an angle θ with the z axis. The probe light beam is bounced back with some lateral displacement covered along the y axis at the interface known as the GHS and symbolized as Δs_r . A coherent control field is considered to irradiate normally on

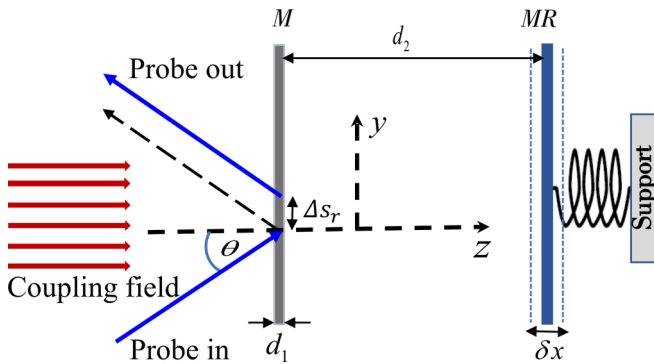


FIG. 1. Schematic for the cavity optomechanical system with external fields. The letters M and MR denote the partially reflecting fixed and perfectly reflecting movable mirrors, respectively. The thickness of the left mirror and the length of the cavity are denoted by d_1 (permittivity ϵ_1) and d_2 (effective permittivity ϵ_2), whereas δx is the mean displacement of MR, and Δs_r is the lateral shift in the reflected probe beam. The coherent coupling field (Ω_L , ω_L) is denoted by the arrows normal to M , and the probe beam (Ω_p , ω_p) is at an incident angle (θ) to the interface.

a semitransparent wall (glass slab) of the cavity for convenience. Without loss of generality, a weak probe beam with TE polarization is also injected to the cavity at some incident angle with normal to the interface. Upon reflection from the interface, the probe light beam suffers a lateral shift along the interface. For the well-collimated probe light beam with sufficiently large width (i.e., under narrow angular-spectrum approximation, $\Delta k \ll k$), the GHS in the reflected light field can be calculated using the stationary phase theory [4,24],

$$\Delta s_r = -\frac{\lambda_p}{2\pi} \frac{d\phi_r}{d\theta}, \quad (1)$$

where λ_p is the wavelength of the incident probe beam and ϕ_r is the phase of the TE-polarized reflection coefficient $R(k_y, \omega_p)$. The final expression for the GHS can be given explicitly as [31]

$$\Delta s_r = -\frac{\lambda_p}{2\pi} \frac{1}{|R|^2} \left\{ \text{Re}[R(\omega_p)] \frac{d \text{Im}[R(\omega_p)]}{d\theta} - \text{Im}[R(\omega_p)] \frac{d \text{Re}[R(\omega_p)]}{d\theta} \right\}. \quad (2)$$

The reflection coefficient used in Eq. (2) can be derived by using the standard characteristic transfer-matrix method [31,44] or by the Fresnel reflection coefficient method [45]. We use the latter one whose details are given in the Appendix. The reflection coefficient expression for the probe light beam is written as

$$R(k_y, \omega_p) = \frac{\cos(k_{1z}d_1)(P_1P_2 + A) + j \sin(k_{1z}d_1)(AP_1 + P_2)}{\cos(k_{1z}d_1)(P_1P_2 - A) + j \sin(k_{1z}d_1)(AP_1 - P_2)}, \quad (3)$$

where $A = [1 + \exp(-2jk_{2z}d_2)]/[1 - \exp(-2jk_{2z}d_2)]$, $P_1 = \mu_1 k_{0z}/(\mu_0 k_{1z})$, and $P_2 = \mu_2 k_{1z}/(\mu_1 k_{2z})$. In Eq. (3), $k_{iz} = k_0 \sqrt{\epsilon_i - \sin^2 \theta}$ and μ_i are the z component of the probe beam's wave number and permeability, respectively, where $i = 0-2$ stands for the i th layers of the media. The relation for the cavity effective permittivity is given by $\epsilon_2 = 1 + \chi_{\text{eff}}(\omega_p)$, which is a function of the probe light field. It should be noted that inside the optomechanical cavity, the cavity field interacts nonlinearly with the MR. So, when external fields are applied to the cavity, the resonant conditions are modified due to the phase changes in the light fields which can be responsible for the dispersion or absorption of the probe light field. Hence, due to the phase changes, the value of $\chi_{\text{eff}}(\omega_p)$ is modified so that it can alter the path of the light field reflecting out of the interface. Now our main focus is to acquire an analytical expression for $\chi_{\text{eff}}(\omega_p)$ to help us find the reflection coefficient for the outgoing probe light beam, through a semiclassical quantum approach.

The total Hamiltonian for our proposed COMS driven by a classical control field and interacted with the weak probe field is given as

$$H_T = \hbar\omega_c c^\dagger c + \frac{1}{2} \hbar\omega_m (x^2 + p^2) + \hbar R_0 c^\dagger c x + i\hbar\Omega_L (c^\dagger e^{-i\omega_L t} - c e^{i\omega_L t}) + i\hbar(c^\dagger \Omega_p e^{-i\omega_p t} - c \Omega_p^* e^{i\omega_p t}). \quad (4)$$

The first term on the right-hand side of Eq. (4) shows the energy of the cavity mode with frequency ω_c , whereas c^\dagger and c are the bosonic creation and annihilation operators of the cavity mode, respectively, satisfying the commutation relation $[c, c^\dagger] = 1$. The second term expresses the energy of the mechanical resonator modeled as a quantum harmonic oscillator at resonance frequency ω_m . Here, x and p are the dimensionless position and momentum operators of MR, respectively. The third term is the expression for optomechanical coupling between the cavity mode and the mechanical mode via the radiation pressure coupling rate R_0 (also known as optomechanical coupling). The last two terms are the external coherent control field and the probe light beam interacting with the cavity mode, respectively. In the rotating frame at control field frequency ω_L , Eq. (4) can be written as

$$H_T = \hbar\Delta_c c^\dagger c + \frac{1}{2}\hbar\omega_m(x^2 + p^2) + \hbar R_0 c^\dagger c x + i\hbar\Omega_L(c^\dagger - c) + i\hbar(c^\dagger\Omega_p e^{-i\Delta_{pc}t} - c\Omega_p^* e^{i\Delta_{pc}t}), \quad (5)$$

where $\Delta_c = \omega_c - \omega_L$ and $\Delta_{pc} = \omega_p - \omega_L$ are the cavity-control and probe-control field detunings, respectively. By using the Heisenberg equation of motion named, here, as the quantum Langevin equation and adding the corresponding damping, dissipation, and fluctuation terms, the equations of motion for MR and the cavity variables can be obtained as follows:

$$\dot{x} = \omega_m p, \quad (6)$$

$$\dot{p} = -\omega_m x - R_0 c^\dagger c - \gamma_m p + \xi(t), \quad (7)$$

$$\dot{c} = -[\gamma_c + i(\Delta_c + R_0 x)]c + \Omega_L + \Omega_p e^{-i\Delta_{pc}t} + \sqrt{2\gamma_c}c_{in}, \quad (8)$$

$$\dot{c}^\dagger = -[\gamma_c - i(\Delta_c + R_0 x)]c^\dagger + \Omega_L + \Omega_p^* e^{i\Delta_{pc}t} + \sqrt{2\gamma_c}c_{in}^\dagger, \quad (9)$$

where γ_c and γ_m denote the radiative decays associated with the cavity and mechanical mode, respectively. Here, the input vacuum noise associated with the cavity field $c_{in}(t)$ has a zero mean value, i.e., $\langle c_{in}(t) \rangle = \langle c_{in}^\dagger(t) \rangle = 0$ obeying a nonvanishing commutation relation [46] $\langle c_{in}(t)c_{in}^\dagger(t') \rangle = \delta(t - t')$. Moreover, the Hermitian Brownian noise operator $\xi(t)$ (also called Langevin thermal force) has zero mean value, that is, $\langle \xi(t) \rangle = 0$ [47]. Taking the derivative of Eq. (6) and substituting Eq. (7) into it, we get the following equation:

$$\ddot{x} + \gamma_m \dot{x} + \omega_m^2 x = -\omega_m R_0 c^\dagger c + \dot{\xi}(t). \quad (10)$$

As we are interested in the mean response of the system to the probe field, we get the mean value linear equations by using factorization assumption $\langle xc \rangle = \langle x \rangle \langle c \rangle$ [43] and dropping the input vacuum noise and Langevin thermal force terms whose mean values are zero. Those equations can be analyzed in the first step by looking for the steady-state solutions $c(t) = c_0$ and $x(t) = x_0$ under the assumption that the coherent control field is much stronger than the probe field ($\Omega_L \gg \Omega_p$) in which all the derivative terms vanish. The steady-state solutions of position and cavity variables are $x_0 = -R_0|c_0|^2/\omega_m$ and $c_0 = \Omega_L/(\gamma_c + i\Delta)$, where $\Delta = \Delta_c + R_0 x_0$ is the effective cavity detuning.

Now, we study the dynamics of small excursions $\delta c(t)$ and $\delta x(t)$ as we have interposed a weak probe field that can impart small fluctuations to the system. So we replace $\langle c(t) \rangle = c_0 + \delta c(t)$ and $\langle x(t) \rangle = x_0 + \delta x(t)$ [48] in Eqs. (8)–(10) to get the linearized equations as

$$\delta\dot{c}(t) = -(\gamma_c + i\Delta)\delta c(t) - iR_0 c_0 \delta x(t) + \Omega_p e^{-i\Delta_{pc}t}, \quad (11)$$

$$\begin{aligned} \delta\dot{c}^\dagger(t) &= \delta\dot{c}^*(t) \\ &= -(\gamma_c - i\Delta)\delta c^*(t) + iR_0 c_0 \delta x(t) + \Omega_p^* e^{i\Delta_{pc}t}, \end{aligned} \quad (12)$$

$$\delta\ddot{x}(t) + \gamma_m \delta\dot{x}(t) + \omega_m^2 \delta x(t) = -\omega_m R_0 [c_0^* \delta c(t) + c_0 \delta c^*(t)]. \quad (13)$$

Equations (11)–(13) can easily be solved in the frequency domain by applying Fourier transform at the probe field frequency as $\delta c(\omega_p) = \int \delta c(t) \exp(-i\omega_p t) dt$ and $\delta x(\omega_p) = \int \delta x(t) \exp(-i\omega_p t) dt$. Therefore, we have

$$\delta c(\omega_p) = \frac{-iG\delta x(\omega_p) + 2\pi\Omega_p D(\omega_p + \Delta_{pc})}{[\gamma_c + i(\Delta - i\omega_p)]}, \quad (14)$$

$$\delta c^*(\omega_p) = \frac{iG\delta x(\omega_p) + 2\pi\Omega_p^* D(\omega_p - \Delta_{pc})}{[\gamma_c - i(\Delta + \omega_p)]}, \quad (15)$$

$$\delta x(\omega_p) = \frac{-\omega_m G[\delta c(\omega_p) + \delta c^*(\omega_p)]}{\omega_m^2 - i\gamma_m \omega_p - \omega_p^2}, \quad (16)$$

where $2\pi D(\omega_p + \Delta_{pc})$ and $2\pi D(\omega_p - \Delta_{pc})$ are the Dirac- δ functions appearing in Eqs. (11) and (12), respectively, due to the presence of exponential terms. By substituting Eqs. (14) and (15) into Eq. (16), we obtain the MR's frequency-dependent position and susceptibility expressions as

$$\delta x(\omega_p) = \frac{2\pi\Omega_p D(2\omega_p - \omega_L) G \chi_{\text{eff}}(\omega_p) [\gamma_c - i(\Delta + \omega_p)] + 2\pi\Omega_p^* D(\omega_L) [\gamma_c + i(\Delta - \omega_p)]}{[(\gamma_c - i\omega_p)^2 + \Delta^2] + iG^2 \chi_{\text{eff}}(\omega_p) [\gamma_c - i(\Delta + \omega_p)]}, \quad (17)$$

$$\chi_{\text{eff}}(\omega_p) = \frac{-\omega_m [\gamma_c - i(\Delta + \omega_p)]}{[\gamma_c - i(\Delta + \omega_p)](\omega_m^2 - i\gamma_m \omega_p - \omega_p^2) + iG^2 \omega_m}. \quad (18)$$

Here in Eq. (18), $\chi_{\text{eff}}(\omega_p)$ is the effective mechanical susceptibility, $\Delta = \Delta_c + R_0 x_0$ is the effective cavity detuning, $x_0 = -R_0|c_0|^2/\omega_m$ and $c_0 = \Omega_L/(\gamma_c + i\Delta)$, respectively,

are the position and cavity mode steady-state values, and $G = R_0 c_0$ is the effective optomechanical coupling. We can write $\chi_{\text{eff}}(\omega_p) = \chi'_{\text{eff}}(\omega_p) + i\chi''_{\text{eff}}(\omega_p)$ because $\chi_{\text{eff}}(\omega_p)$ is a

complex expression containing real and imaginary terms accountable for the dispersive-absorptive properties of the probe beam, respectively.

III. RESULTS AND DISCUSSION

We consider the following parameters with fixed values in order to demonstrate the manipulation of the GHS in our system: $\epsilon_0 = 1$, $\epsilon_1 = 2.22$, $\mu_0 = \mu_1 = \mu_2 = 1$, $c = 3 \times 10^8$ m/s, $d_1 = 0.2 \mu\text{m}$, $d_2 = 5 \mu\text{m}$, $\omega_m/2\pi = 10^8$ Hz, $\gamma_c = 0.2\omega_m$, $\gamma_m = \omega_m/6700$, and $\omega_p/2\pi = 300$ THz. In this section, we discuss the effect of coherent control field strength and various system parameters on the GHS manipulation. The cavity responds very sensitively to the optomechanical coupling, effective cavity detuning, and to the cavity decay rate, which are responsible for enhanced manipulation of the GHS at different incidence angles.

A. Impact of control field on the GHS

Figure 2 shows the reflection coefficient and the GHS plotted against incident angle of the probe beam in which we witness the manipulation of both quantities under different strengths of the control field. In Fig. 2(a), the absorption dips can be seen at certain incident angles of the probe field where resonance conditions occur. The GHS peaks pop up where the probe field is absorbed due to the imaginary term of χ_{eff} shown in Fig. 2(b). For lower values of the control field, the shift is negative, and its magnitude is very small, but for a larger value of the control field, we observe both positive and negative shifts with considerable enhancement. The larger value of the control field results in full probe field absorption at the resonance condition, which leads to a negative enhanced shift peak. Actually, a large amount of coherent control field modifies the value of χ_{eff} owing to the phase change in the field inside the cavity as a result of which we can see both positive and negative shifts of the reflected probe light beam. Thus, by tuning the control field, we can control the phase changes and so does the manipulation of the GHS. The insets in Fig. 2(b) are drawn to enlarge the peaks having small values and make it more visible.

B. Effect of cavity length on the GHS

Some earlier works [14,24,49] have revealed that the GHS behavior strongly depends upon the cavity length. We also expect a modification in the GHS behavior by changing the cavity length in our case. In Figs. 3(a) and 3(c), two different cavity lengths have been used to observe the behavior of reflection coefficient of the probe beam and the GHS, respectively. When the cavity length is changed to $d_2 = 4 \mu\text{m}$, we note the shift peaks switched from positive to large negative values with a decrease in the peaks number. For a relatively larger value of cavity length, i.e., $d_2 = 6 \mu\text{m}$, the shift remains negative but with relatively lower strength. Also, the reflection coefficient dips where the resonance conditions occur, get increased in number. In Fig. 3(b), the phase plot corresponding to the reflected beam is shown where the phase changes can clearly be seen at the points where the dips of reflection coefficient occur [see Fig. 3(a)]. Similarly, large GHSs can be observed at the angles where the phase changes occur due

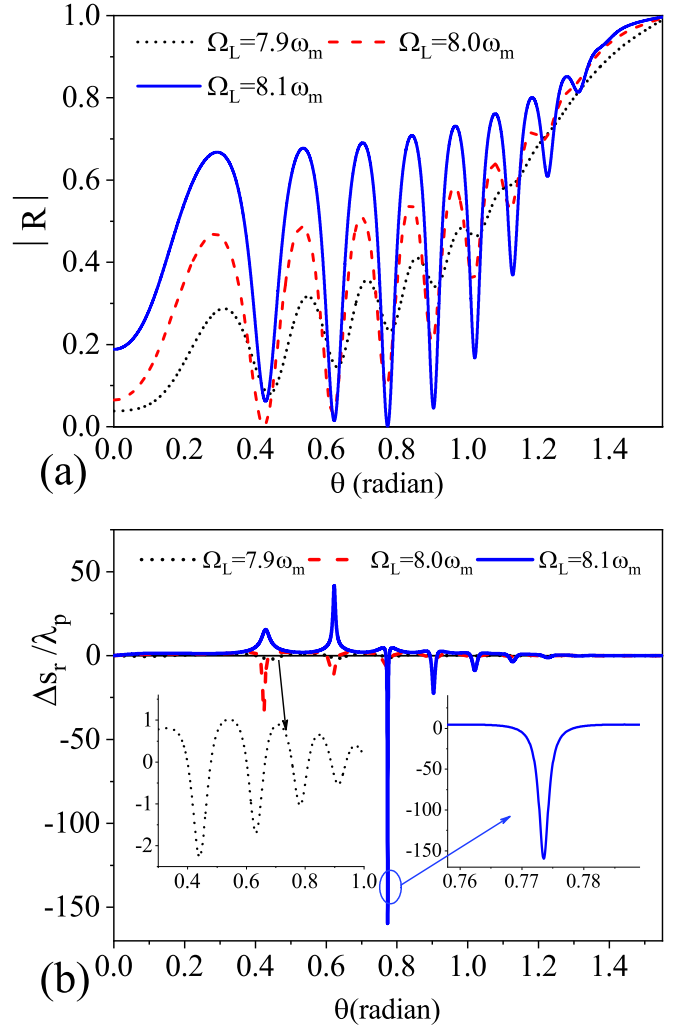


FIG. 2. (a) The reflection coefficient ($|R|$) and (b) the GHS ($\Delta s_r/\lambda_p$) as a function of incident angle θ . The general parameters are $\omega_m/2\pi = 10^8$ Hz, $R_0 = 0.72\omega_m$, $\epsilon_1 = 2.22$, $\mu_0 = \mu_1 = \mu_2 = 1$, $c = 3 \times 10^8$ m/s, $d_1 = 0.2 \mu\text{m}$, $d_2 = 5 \mu\text{m}$, $\omega_p/2\pi = 300$ THz, $\gamma_c = 0.2\omega_m$, and $\gamma_m = \omega_m/6700$.

to changing the cavity length. In the same fashion, both the positive and the negative shifts come into play due to the phase changes at certain incident angles. Thus, by changing the cavity length, the behavior of the GHS can be tuned significantly from positive to negative in addition to changing the number of resonances which happen due to the phase changes.

C. Effect of the quantum parameter on the GHS

A slight change in the optomechanical coupling (also known as the quantum parameter in some places [50]) can modify the resonance condition which means that optomechanical coupling is very sensitive to the manipulation of the GHS. Figure 4 shows the dependency of the GHS on the quantum parameter under different incident angles. Figures 4(a) and 4(b) have been plotted for $\theta = 30^\circ$, 52° whereas in Figs. 4(c) and 4(d), the curves shown are plotted at 76° . In Fig. 4(a), the resonance dips at a certain incident angle

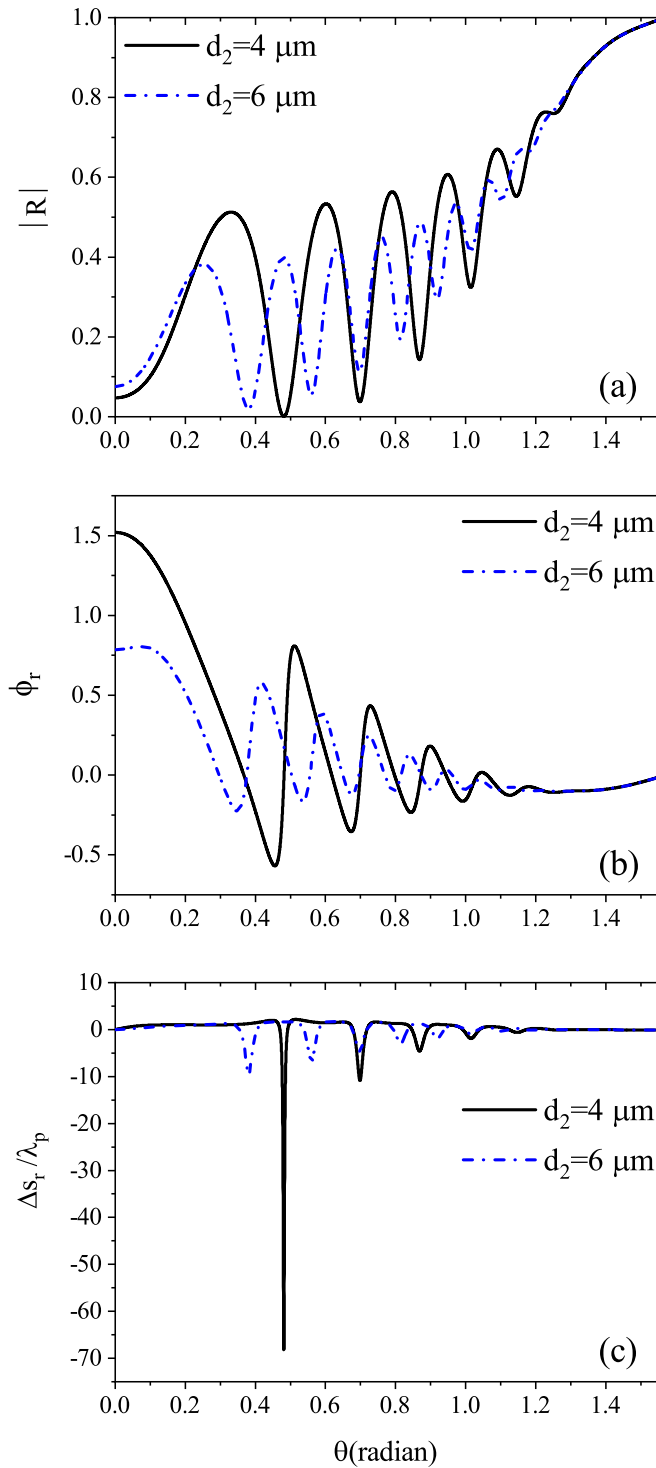


FIG. 3. (a) The reflection coefficient, (b) phase ϕ_r , of the reflected field, and (c) the GHS as a function of incident angle θ . Here, the control field strength is $\Omega_L = 8.1\omega_m$, whereas all other parameters are the same as in Fig. 2.

along the x axis can modify the GHS value from positive to almost zero, following an abrupt change and then goes high until it becomes constant. In Fig. 4(b), we note a negative peak for the GHS, which then turns to a highly enhanced positive peak in the reflected probe light beam. The reason for these

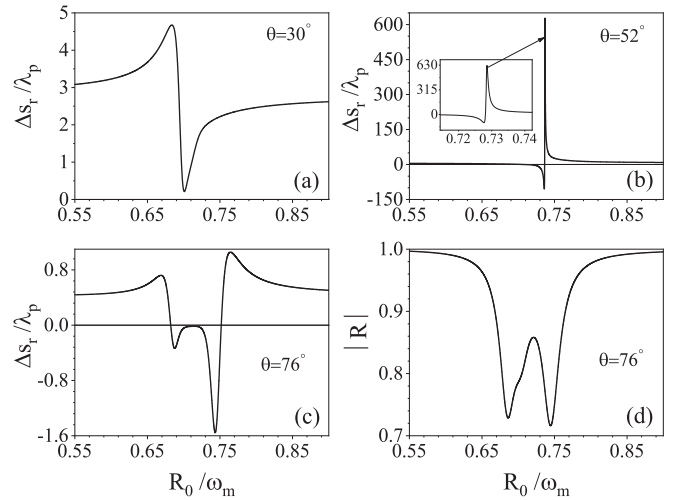


FIG. 4. The dependence of the GHS on the normalized quantum parameter R_0 / ω_m when (a) $\theta = 30^\circ$, (b) $\theta = 52^\circ$, and (c) $\theta = 76^\circ$. (d) The reflection coefficient as a function of normalized quantum parameter R_0 / ω_m at $\theta = 76^\circ$. The control field strength is fixed at $\Omega_L / \omega_m = 8.0$. All the other parameters are same as in Fig. 2.

changing natures of peaks from negative to positive is due to the abrupt change in the phase of the field inside the cavity by changing the optomechanical coupling. The inset shows how the peak goes from a negative to a positive peak. At this angle, the maxima at both negative and positive peaks represent a great enhancement of the shift. It is seen that changing the quantum parameter can flexibly manipulate the GHS at different angles with a large controllable range. Here, this enhancement comes into account because of the probe's beam absorption at the resonance point. Figures 4(c) and 4(d) show the GHS and the reflection coefficient, respectively, at the probe reflected beam. The GHS shows two negative peaks at resonance points as shown in the reflection coefficient graph (two small dips). Hence, by keeping the control field fixed, we see the absorption dips at resonance points for a range of optomechanical coupling values at which positive as well as negative GHSs are noticed.

D. Dependence of effective cavity detuning on the GHS

Figure 5 shows the dependence of the GHS on the effective cavity detuning, and we can see the manipulation effect on the GHS owing to effective cavity detuning under different strengths of control field. In Fig. 5(a), no GHS peak is observed when the control field strength is kept zero, which means that there is no influence of the control field on the cavity, and likewise no resonance conditions are matched. By increasing the strength of the control field, an increase in the GHS can be detected. So, the control field can be used as a knob to switch the cavity on and off for the manipulation of the GHS. In Fig. 5(b), we plot the dependence of the GHS on effective cavity detuning under different incident angles of the probe light beam. It can be seen that, at incident angles $\theta = 30^\circ$ and $\theta = 76^\circ$, the magnitude of the GHS is positive and small, but at $\theta = 52^\circ$, the shift is considerably large and follows a steep peak from positive to negative. The reason for this abrupt change is the matching of the resonant condition

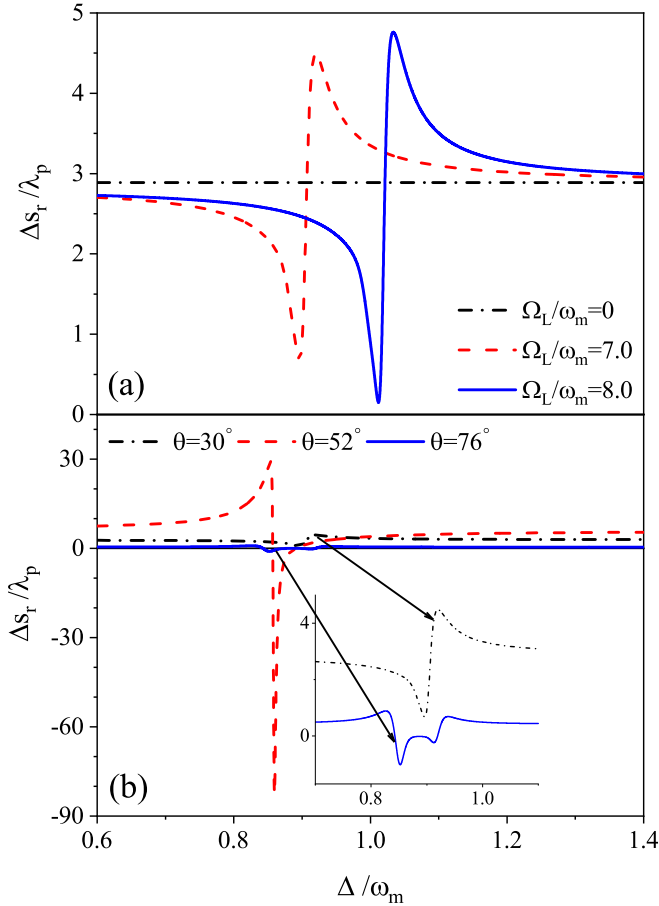


FIG. 5. (a) The GHS as a function of normalized effective cavity detuning Δ / ω_m under different control field strengths Ω_L with a fixed $\theta = 30^\circ$. (b) The GHS as a function of normalized effective cavity detuning Δ / ω_m under different incident angles θ with a fixed $\Omega_L / \omega_m = 7.0$. All the other parameters are same as in Fig. 2.

where the large probe beam absorption has occurred at that point along a range of effective cavity detuning. Thus, the control field plays a vital role in controlling the GHS at a range of effective cavity detuning values, and the GHS can be enhanced significantly by choosing a certain incident angle.

E. Effect of the cavity decay rate on the GHS

Indeed, our COMS is a lossy one because of the presence of the semireflecting mirror from where the external fields go in and out of the cavity. Therefore, the cavity photons have a limited lifetime after which they decay (lose energy) at a rate named as the cavity decay rate γ_c . The cavity decay rate may be different for the optical cavities with a changed Q factor. The $\gamma_c \propto 1/\tau_c$ (τ_c is the lifetime) of the cavity photons, so it can also affect the reflection coefficient, and so does the GHS of the reflected probe light beam. Figure 6(a) shows the behavior of the reflection coefficient against the normalized cavity decay rate under different control field strengths. It can be seen that with the increase in cavity decay rate, the reflection coefficient decays down from its maximum value. For different control field strengths, the decaying quantity is different, but the overall picture is the same, which is, the

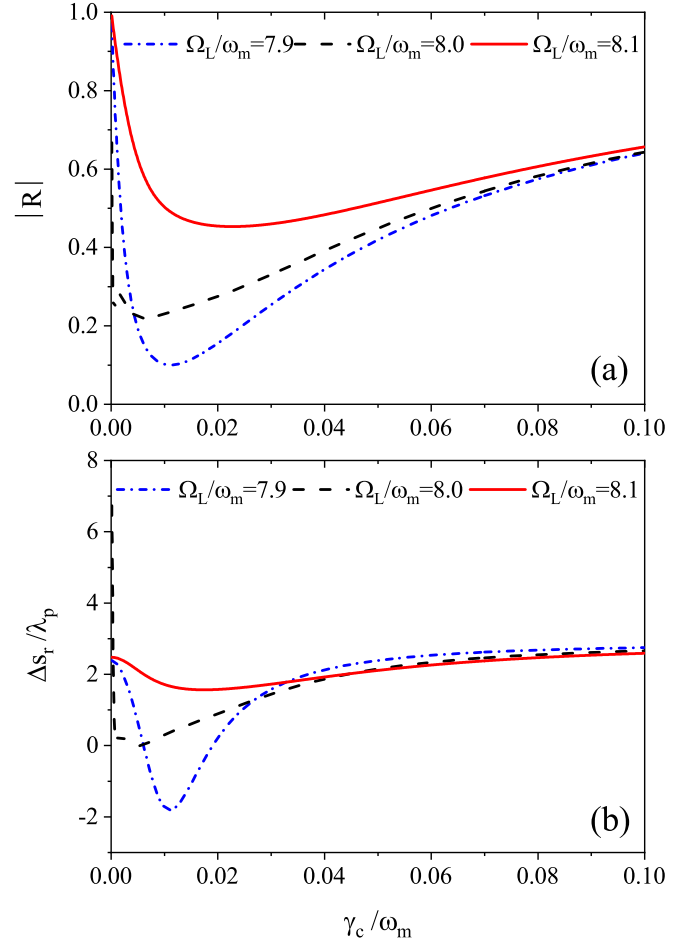


FIG. 6. (a) The reflection coefficient and (b) the GHS as a function of normalized cavity decay rate γ_c / ω_m at $\theta = 30^\circ$. All the other parameters are the same as in Fig. 2.

resonant conditions are disturbed, and we do not see any significant dip of probe absorption. The GHS is significantly suppressed for lower values of Ω_L at a certain range of cavity decay rate as can be seen in Fig. 6(b). The reason for such suppression is the increasingly decaying behavior of cavity photons, which reduce the optomechanical coupling between the cavity field and the mechanical mode. However, for a larger range of γ_c / ω_m , the GHS shows a converging behavior. The reason behind this convergence is that, when the cavity decay rate γ_c increases, initially, we see a suppression in the GHS curves. As γ_c further increases, the photon loss is considerably high due to which the shift should further suppress, but the strong control field strength Ω_L is continuously injecting photons into the cavity so that a stable interaction between the cavity mode and the mechanical mode is established and so the GHS converges to a fixed value.

IV. SUMMARY

We have theoretically investigated the GHS in a cavity optomechanical system excited by a coherent control field and noted the manipulation of the GHS by the control field. By tuning the control field, we have detected positive as well as negative GHS peaks at the absorption dips depending upon

the strength of the control field used. By modifying the cavity length, we have revealed the behavior of the GHS changing from positive to negative. The cavity decay rate also has a manipulation effect on the GHS, and moreover, we have found a suppression of the GHS with increasing the cavity decay rate at a certain range. We also have observed the convergence of the GHS for a larger range of the cavity decay rate. This proposal motivates one to investigate the GHS experimentally as it could open a window for the researchers to find new exciting phenomena in cavity optomechanical systems.

ACKNOWLEDGMENTS

This research was supported by the National Natural Science Foundation of China (Grants No. 11674284, No. 11974309, No. 11974311, and No. U1801661), Zhejiang Provincial Natural Science Foundation of China under Grant No. LD18A040001, the National Key Research and Development Program of China (Grant No. 2017YFA0304202), and the Fundamental Research Funds for the Center Universities (Grant No. 2019FZA3005).

APPENDIX: THE FRESNEL EQUATION METHOD

We explain briefly Maxwell's equations both for incident and reflected TE-polarized electromagnetic waves by matching boundary conditions at the interfaces. The incident and reflected electric-field expressions at the air-glass slab interface, i.e., $z < 0$ are given by

$$E_i = \hat{x}E_0 e^{j(k_{0z}z + k_{0y}y)}, \quad (\text{A1})$$

$$E_r = \hat{x}RE_0 e^{j(-k_{0z}z + k_{0y}y)}. \quad (\text{A2})$$

Similarly, the incident and reflected magnetic-field expressions at the interface, i.e., $z < 0$ are written as

$$H_i = \frac{1}{\omega\mu_0} (-\hat{y}k_{0z} + \hat{z}k_{0y})E_0 e^{j(k_{0z}z + k_{0y}y)}, \quad (\text{A3})$$

$$H_r = \frac{1}{\omega\mu_0} (\hat{y}k_{0z} + \hat{z}k_{0y})RE_0 e^{j(-k_{0z}z + k_{0y}y)}, \quad (\text{A4})$$

where $\vec{k}_i = \hat{z}k_{0z} + \hat{y}k_{0y}$ is the wave vector of the incident probe wave field with $k_{0z} = k \cos \theta$ and $k_{0y} = k \sin \theta$ the z and y components, respectively, and $k = \omega_p/c$ is the wave number

of the plane wave in vacuum. The transmitted electric and magnetic fields at $z > 0$, respectively, are given as

$$E_2 = \hat{x}E_1^+ E_0 e^{j(k_{1z}z + k_{1y}y)} + \hat{x}E_1^- E_0 e^{j(-k_{1z}z + k_{1y}y)}, \quad (\text{A5})$$

$$H_2 = \frac{1}{\omega\mu_1} (-\hat{y}k_{1z} + \hat{z}k_{1y})E_1^+ E_0 e^{j(k_{1z}z + k_{1y}y)} + \frac{1}{\omega\mu_1} (\hat{y}k_{1z} + \hat{z}k_{1y})E_1^- E_0 e^{j(-k_{1z}z + k_{1y}y)}, \quad (\text{A6})$$

where $\vec{k}_r = -\hat{z}k_{0z} + \hat{y}k_{0y}$ is the wave vector of the reflected beam. The electromagnetic field enters the cavity and reflects back off the cavity wall which is a perfect electric conductor (PEC). The electric and magnetic-field expressions at the PEC interface are written as

$$E_3 = \hat{x}E_2^+ E_0 e^{j(k_{2z}z + k_{2y}y)} + \hat{x}E_2^- E_0 e^{j(-k_{2z}z + k_{2y}y)}, \quad (\text{A7})$$

$$H_3 = \frac{1}{\omega\mu_2} (-\hat{y}k_{2z} + \hat{z}k_{2y})E_2^+ E_0 e^{j(k_{2z}z + k_{2y}y)} + \frac{1}{\omega\mu_2} (\hat{y}k_{2z} + \hat{z}k_{2y})E_2^- E_0 e^{j(-k_{2z}z + k_{2y}y)}. \quad (\text{A8})$$

By using the dielectric and the PEC boundary conditions, one can get the desired reflection coefficient, i.e., Eq. (3) for the probe light beam. At boundary condition $z = 0$, Eqs. (A3)–(A6) can be solved to get the result as

$$e^{jk_{0y}y}(1 + R) = e^{jk_{1y}y}(E_1^+ + E_1^-). \quad (\text{A9})$$

$$\frac{k_{0z}}{\mu_0} e^{jk_{0y}y}(1 - R) = \frac{k_{1z}}{\mu_1} e^{jk_{1y}y}(E_1^+ - E_1^-). \quad (\text{A10})$$

We apply boundary conditions at $z = d_1$ where the total electric and magnetic fields must be continuous, which results in the expressions below,

$$e^{jk_{1y}y}(E_1^+ e^{jk_{1z}d_1} - E_1^- e^{-jk_{1z}d_1}) = e^{jk_{2y}y}(E_2^+ e^{jk_{2z}d_1} - E_2^- e^{-jk_{2z}d_1}), \quad (\text{A11})$$

$$\frac{k_{1z}}{\mu_1} e^{jk_{1y}y}(E_1^+ e^{jk_{1z}d_1} - E_1^- e^{-jk_{1z}d_1}) = \frac{k_{2z}}{\mu_2} e^{jk_{2y}y}(E_2^+ e^{jk_{2z}d_1} - E_2^- e^{-jk_{2z}d_1}). \quad (\text{A12})$$

At $z = d_2$, the expression E_2^+ from Eqs. (A7) and (A8) can be obtained as

$$E_2^+ = -E_2^- e^{-2jk_{2z}(d_1 + d_2)}. \quad (\text{A13})$$

Now, we solve Eqs. (A9)–(A13) by using simple but lengthy algebra to get the reflection coefficient for the TE-polarized electromagnetic wave shown in Eq. (3).

-
- [1] J. Picht, *Ann. Phys. (Paris)* **395**, 433 (1929).
 [2] F. Goos and H. Hanchen, *Ann. Phys.* **436**, 333 (1947).
 [3] F. Goos and H. L. Hanchen, *Ann. Phys.* **440**, 251 (1949).
 [4] K. V. Artmann, *Ann. Phys. (Leipzig)* **437**, 87 (1948).
 [5] R. H. Renard, *J. Opt. Soc. Am.* **54**, 1190 (1964).

- [6] X. Wang, C. Yin, J. Sun, H. Li, M. Sang, W. Yuan, Z. Cao, and M. Huang, *Appl. Phys. Lett.* **103**, 151113 (2013).
 [7] Y. Wang, H. Li, Z. Cao, T. Yu, Q. Shen, and Y. He, *Appl. Phys. Lett.* **92**, 061117 (2008).
 [8] T. Hashimoto and T. Yoshino, *Opt. Lett.* **14**, 913 (1989).

- [9] C. W. Huse and T. Tamir, *J. Opt. Soc. Am. A* **2**, 978 (1985).
- [10] Y. Song, H. C. Wu, and Y. Guo, *Appl. Phys. Lett.* **100**, 253116 (2012).
- [11] C. W. Chen, W. C. Lin, L. S. Liao, Z. H. Lin, H. P. Chiang, P. T. Leung, E. Sijercic, and W. S. Tse, *Appl. Opt.* **46**, 5347 (2007).
- [12] *Integrated Optics*, edited by T. Tamir (Springer, Berlin, 1979).
- [13] Y. Wang, Z. G. Yue, Y. H. Liu, and J. W. Xu, *Optik* **121**, 307 (2010).
- [14] L. G. Wang, H. Chen, and S. Y. Zhu, *Opt. Lett.* **30**, 2936 (2005).
- [15] H. Wang, Z. Zhou, and H. Tian, *Appl. Phys. B: Lasers Opt.* **99**, 513 (2010).
- [16] Y. Yan, X. Chen, and C.-F. Li, *Phys. Lett. A* **361**, 178 (2007).
- [17] I. V. Shadrivov, A. A. Zharov, and Y. S. Kivshar, *Appl. Phys. Lett.* **83**, 2713 (2003).
- [18] D. K. Qing and G. Chen, *Opt. Lett.* **29**, 872 (2004).
- [19] P. R. Berman, *Phys. Rev. E* **66**, 067603 (2002).
- [20] X. Chen and C. F. Li, *Phys. Rev. E* **69**, 066617 (2004).
- [21] L. G. Wang and S. Y. Zhu, *Appl. Phys. Lett.* **87**, 221102 (2005).
- [22] L. G. Wang and S. Y. Zhu, *Opt. Lett.* **31**, 101 (2006).
- [23] D. Felbacq, A. Moreau, and R. Smaïli, *Opt. Lett.* **28**, 1633 (2003).
- [24] C. F. Li, *Phys. Rev. Lett.* **91**, 133903 (2003).
- [25] A. Alù, M. G. Silveirinha, A. Salandrino, and N. Engheta, *Phys. Rev. B* **75**, 155410 (2007).
- [26] R. Liu, Q. Cheng, T. Hand, J. J. Mock, T. J. Cui, S. A. Cummer, and D. R. Smith, *Phys. Rev. Lett.* **100**, 023903 (2008).
- [27] S. Feng, *Phys. Rev. Lett.* **108**, 193904 (2012).
- [28] S. Feng and K. Halterman, *Phys. Rev. B* **86**, 165103 (2012).
- [29] W. Jisen, J. Zhang, L. G. Wang, and S. Y. Zhu, *J. Opt. Soc. Am. B* **34**, 2310 (2017).
- [30] M. O. Scully, *Phys. Rev. Lett.* **67**, 1855 (1991).
- [31] L. G. Wang, M. Ikram, and M. S. Zubairy, *Phys. Rev. A* **77**, 023811 (2008).
- [32] Ziauddin, S. Qamar, and M. S. Zubairy, *Phys. Rev. A* **81**, 023821 (2010).
- [33] J.-N. Su, W.-W. Deng, and G.-X. Li, *Acta. Phys. Sin* **61**, 144210 (2012).
- [34] B. A. Bacha, A.-U. Rahman, A. Iqbal, and N. Khan, *Phys. Lett. A* **383**, 781 (2019).
- [35] W. W. Deng, S. P. Wu, and G. X. Li, *Opt. Commun.* **285**, 2668 (2012).
- [36] C. Genes, A. Mari, D. Vitali, and P. Tombesi, *Adv. At., Mol., Opt. Phys.* **57**, 33 (2009).
- [37] F. Marquardt and S. M. Girvin, *Physics* **2**, 40 (2009).
- [38] I. Favero and K. Karrai, *Nat. Photonics* **3**, 201 (2009).
- [39] T. J. Kippenberg and K. J. Vahala, *Opt. Express* **15**, 17172 (2007).
- [40] M. Aspelmeyer, P. Meystre, and K. Schwab, *Phys. Today* **65**(7), 29 (2012).
- [41] P. Lebedew, *Ann. Phys. (Leipzig)* **311**, 433 (1901).
- [42] E. F. Nichols and G. F. Hull, *Phys. Rev. (Series I)* **13**, 307 (1901).
- [43] G. S. Agarwal and S. Huang, *Phys. Rev. A* **81**, 041803(R) (2010).
- [44] M. Born and E. Wolf, *Principles of Optics* (Cambridge University Press, Cambridge, UK, 1999).
- [45] J. A. Kong, B.-I. Wu, and Y. Zhang, *Appl. Phys. Lett.* **80**, 2084 (2002).
- [46] W. Gardiner and P. Zoller, *Quantum Noise* (Springer-Verlag, Berlin, 2000).
- [47] C. Genes, D. Vitali, and P. Tombesi, *Phys. Rev. A* **77**, 050307(R) (2008).
- [48] G. S. Agarwal, *Quantum Optics* (Cambridge University Press, Cambridge, UK, 2013).
- [49] M. Cheng, Y. Zhou, Y. Li, and X. Li, *J. Opt. Soc. Am. B* **25**, 773 (2008).
- [50] H. Xiong and Y. Wu, *Appl. Phys. Rev.* **5**, 031305 (2018).